https://doi.org/10.15407/ufm.24.01.173

F. BAHFIE [1,*], A. MANAF [2,], W. ASTUTI [1,***], F. NURJAMAN [1], E. PRASETYO [1,3], Y. TRIAPRIANI [1], and D. SUSANTI [4]**

[1] Research Centre of Mining Technology,
National Research and Innovation Agency of Indonesia,
South Lampung, 35361 Lampung, Indonesia
[2] Physics Department, Faculty of Mathematics and Science,
University of Indonesia,
16424 Depok, West Java, Indonesia
[3] Department of Chemical Engineering,
Norwegian University of Science and Technology,
7491 Trondheim, Norway
[4] Department of Metallurgical and Material Engineering,
Faculty of Industrial Technology and Systems Engineering,
Institut Teknologi Sepuluh Nopember,
60111 Surabaya, East Java, Indonesia

* fath007@brin.go.id, ** azwar@ui.ac.id, *** widi.mineral@gmail.com

FROM NICKEL ORE TO Ni NANOPARTICLES IN THE EXTRACTION PROCESS: PROPERTIES AND APPLICATION

Laterite nickel ore is a mineral rock, which contains iron–nickel oxide compounds. One processing technology proposed to treat the ore is the Caron process. In general, the Caron process combines pyrometallurgical and hydrometallurgical stages. In the pyrometallurgical step, the ore mixed with reductant is heated up to 1800 °C in a rotary kiln-electric furnace to transform iron–nickel oxide into iron–nickel alloy. In the hydrometallurgical stage, nickel has to be dissolved selectively using ammonia solution (alkaline). The further process is aimed to separate and purify the nickel in

Citation: F. Bahfie, A. Manaf, W. Astuti, F. Nurjaman, E. Prasetyo, Y. Triapriani, and D. Susanti, From Nickel Ore to Ni Nanoparticles in the Extraction Process: Properties and Application, *Progress in Physics of Metals*, **24**, No. 1: 173–196 (2023)

ammonia solution using solvent extraction and precipitation. The disadvantages of the pyrometallurgical stage in the Caron process include high-energy consumption, low economic value, and technical problems such as partially melted material, which hinders the further process. While in the hydrometallurgical stage, the extensive use of ammonia causes an environmental impact. Selective reduction is proposed to solve problems in the pyrometallurgical stage. Selective reduction is a process favouring the formation of iron oxide to obtain high nickel content in an intermediate product with less energy consumption. An additive is added to the ore to reduce selectively the nickel and decrease the reaction temperature. To solve the environmental impact of ammonia, a novel and safer chemical is proposed as a substitute — the monosodium glutamate (MSG). Selective reduction combined with alkaline leaching using MSG is proposed as an alternative to the Caron method. Precipitation is employed further to purify the nickel that results in nickel nanoparticles with 90–95 wt.% purity.

Keywords: laterite, Caron method, purification, synthesis, nickel nanoparticles.

1. Introduction

Nickel is an essential nonferrous metal and is widely used for stainless steel and alloy steel, steel plating, or catalysts in the hydrogenation process of the petroleum chemical industry [1, 2]. Current nickel resources include nickel sulphide ore and nickel laterite ore composed of oxidized and silicate ores, which account for approximately 30% and 50% of the world's nickel reserves. However, more than 60% of nickel production comes from nickel sulphide ores because nickel in sulphide ores can be easily enriched and recovered by conventional flotation and magnetic and gravitational separations [3]. As high-grade nickel sulphide ores are exploited first and depleted, laterite nickel ores with low nickel grades become gradually the main nickel production resource [4–7]. Nickel in laterite ores mainly occurs in clay minerals (serpentine, smectites, vermiculites, *etc.*) and other silicates such as olivines and pyroxenes or iron oxide minerals. Nickel is enriched as isomorphic substitutions in the lateritic ores during the weathering of ultramafic rocks [8, 9]; therefore, the nickel cannot be extracted by conventional separation. In addition, nickel laterite ore profile has low nickel content and is classified into two layers, such as limonitic and saprolitic [10, 11]. There are two significant developmental advantages for nickel laterite ores: abundant reserves and surface deposits, which can be mined from the surface [12, 13]. Therefore, profitable processing processes for the efficient utilization of laterite nickel ore should be considered and studied [1, 14]. The set out processes for pre-concentration of nickel laterite ores, such as removing coarse fractions from feed, sink-float separation, gravity separation, magnetic separation, electrostatic separation, and flotation prior to hydrometallurgical and pyrometallurgical processes [15].

Nickel laterite and sulphide processes have been carried out [14–16]. Descriptions of individual operations and processes have been provided in various symposia and processes [1, 7–13]. Various flowsheets are used to process laterite ores, generally divided into pyrometallurgical and hydrometallurgical processes. Most pyrometallurgical processes (ferronickel and matte smelting) use conventional flowsheets involving drying, calcining/reduction and electric furnace smelting. The common hydrometallurgical processes are the Caron process and the high-pressure acid leaching (HPAL) process. The Caron process has several weaknesses. The pyrometallurgical process involves drying, calcination and reduction and requires high energy with low percentage nickel formation and the presence of impurities.

The hydrometallurgical process in Caron applies a variety of reagents, and the nickel and cobalt recovery is lower than the HPAL process [17]. The HPAL process requires a predominantly limonitic ore with lower Mg content (<4%). Higher Mg content requires higher acid consumption. In addition, there are that affect the nickel precipitation process in nickel extraction, which the phase form and the laterite mixture between limonite and saprolite. From these factors, the mixing function can minimize the extraction process by Caron. By varying the weight ratio between limonite and saprolite, it is possible to control the amount of iron in limonite and the percentage of magnesium and aluminium in saprolite. Several extraction factors in laterite need to be developed to meet the demand for increasing nickel grades and effective laterite nickel ore exploitation.

In this paper, we review the current status and studies on the development of hydrometallurgical and pyrometallurgical processes by Caron and other hydro- and pyroprocesses for comparison.

2. Hydrometallurgical Processes

Hydrometallurgical processes in nickel laterite ore processing include the Caron process, acid leaching, MSG leaching, and purification of leached extraction. This paper will compare the hydrometallurgical method on Caron and other processes. However, the process cannot tolerate higher amounts of Mg than the pressure acid leaching (PAL) process, for example Nicaro, Punta-Gorda, Yabulu, Nonoc (now closed). The Caron process suffers from several disadvantages in hydrometallurgy, which requires a variety of reagents. The recovery of nickel and cobalt is lower than that of the smelting process or the HPAL process, so modifications to the process are required for the green approach [18].

2.1. Ammonia-Roasting Reduction

The ammonia-roasting reduction was initially defined as the Caron process. The process is shown in Fig. 1, which is primarily suitable for li-

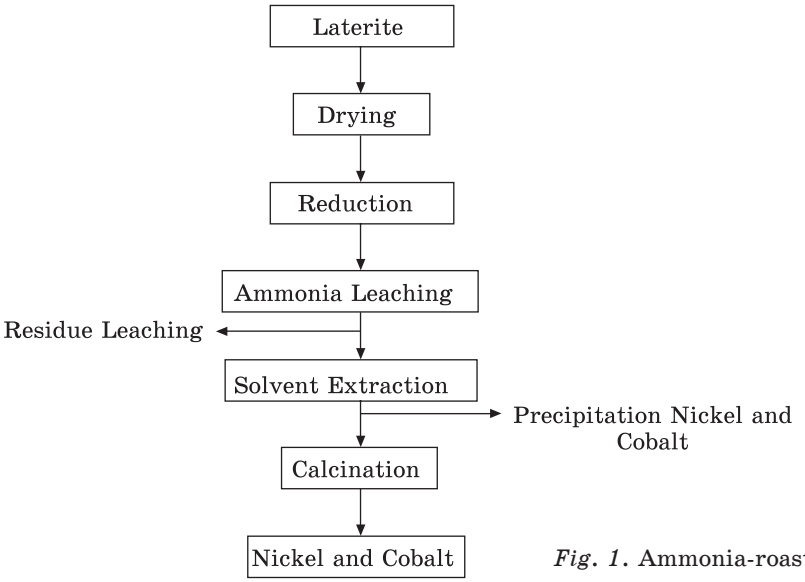

Fig. 1. Ammonia-roasting process

monite ore at a roasting temperature of 700–800 °C with reducing agents. The addition of ammonium carbonate from the roasted product can yield 7.5–8.0 wt.% Ni and 40–50 wt.% Co. The extraction conditions for nickel and cobalt from low-grade laterite ores (Ni 1.17%, Fe 45.56%) using a combined ammonia-roasting leaching method. The optimum conditions based on the study were reductant mass fraction of 10%, roasting time of 120 minutes and roasting temperature of 750–800 °C. In the ammonia leaching process, the liquid–solid ratio is 4:1 (ml/g), the leaching temperature is 40 °C, the leaching time is 120 minutes, and the concentration ratio of NH_3 to CO_2 is 90 g/l and 60 g/l. Under optimal conditions, the leaching efficiency of nickel and cobalt is 86.25% and 60.84%, respectively [16]. The elemental sulphur (S) could reduce the processing temperature to 600 °C. The study resulted in higher Ni recovery from limonite and saprolite ores. The addition of 5% S in the roasting process resulted in 98% recovery of Ni from saprolite ore and 80.6% recovery of Ni from limonite ore. Without the addition of S, the recovery of Ni was 28% and 29% for saprolite and limonite ore, respectively, at 600 °C [19]. The optimization of the screening process before combustion can be used on Fe-rich laterites with a large amount of iron (48.3% by weight) and a low amount of nickel (1.04% by weight). The purpose of the screening was to remove some of the silicate minerals from the limonite laterite ore from the Philippines with low recovery. This process increased the nickel and cobalt extraction from 84.0% and 35.5% to 87.9% and 47.4%, respectively. The screening process is used for comprehensive recovery and utilization of

iron content, thereby increasing the iron content in the leaching residue by up to 60.7% [20].

Ni and Co can be extracted simultaneously by reducing roasting-ammonia leaching. However, the recovery rates for nickel and cobalt are relatively low, 7.5–8.0 wt.% Ni and 40–50 wt.% Co. In addition, the reduction leaching process with ammonia cannot be used to extract laterite ores containing high copper, because copper can form complex compounds with ammonia causing very poor separation with nickel and cobalt. Third, this process cannot be used to refine laterite ores that contain high silicon and magnesium levels. Compared to other hydrometallurgical processes for laterite ores, the disadvantage of ammonia leaching is the high-energy consumption due to the roasting process.

2.2. Acid Leaching

There are two types of acid leaching: high-pressure acid leaching and acid leaching. Acid pressure leaching mainly includes pulp preparation, leaching, and recovery of nickel and cobalt from the leach solution. At 250–270 °C and high pressures of 4–5 MPa, this requires expensive equipment maintenance and process condition control costs. The whole process is depicted in Fig. 2. The principle of the acid leaching process under pressure is that nickel and cobalt dissolve into acid under high pressure and high temperature. In general, acid leaching under pressure is carried out in a high acid system, where the free acid of 25–100 g/l can remain in the final liquid; so, the nickel and cobalt extraction is higher than 90%. Under high-pressure and high-temperature conditions, nickel and cobalt extraction will have high levels. Meanwhile, it cannot be used to treat laterite ores with high magnesium because magnesium will increase acid consumption by high reactivity of magnesium with the acid.

The most frequently used acid is sulphuric acid [21–23]. As Ref. [22] reports, the extraction of nickel from laterite ores is enhanced by increasing the molarity of the acid or the addition of a small amount of soluble sodium. When the acid load

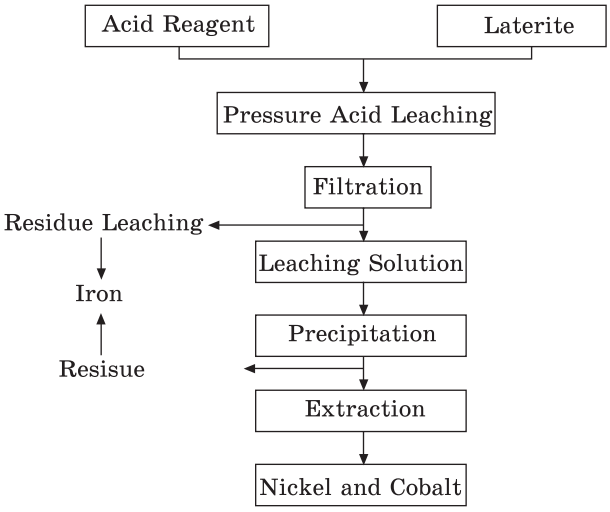

Fig. 2. High-pressure acid leaching

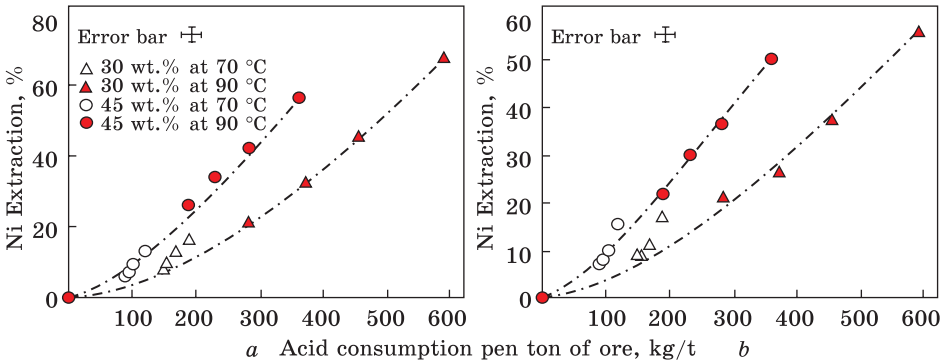

Fig. 3. Acid consumption *vs.* Ni (*a*) and Co (*b*) extraction of 30 and 45 wt.% siliceous goethite (SG) slurries for 4 hours, leaching at pH 1 and temperatures of 70 and 90 °C [26, 27]

is 380 kg/ton of ore, the nickel and cobalt content produced is 93.3% and 91.6%, respectively. Meanwhile, in a solution with sodium ion conditions of 5 g/l with an acid charge of 320 kg/ton ore, nickel and cobalt yields are 93.6% and 95.2%, respectively. The results show that 15% less acid could obtain the same nickel extraction from laterite ore in a solution containing 5 g/l sodium ions compared to the same extraction using a higher acid concentration. In addition, kinetic studies are an essential part of the sulphuric acid pressure leaching. The leaching kinetics of limonite ore, which mainly consisted of maghemite and magnetite, is using high-pressure sulphuric acid leaching. It was found that the leaching kinetics followed a shrinking core model in the initial and intermediate studies, while it also adhered to the acid diffusion control in later stages [24]. Different kinetic models correspond to different laterite minerals. The pressurized nitric acid leaching and used sulphuric acid leaching to extract nickel and cobalt from Indonesian limonite ore, consisting mainly of goethite and magnetite. The optimal conditions were as follow: acid/ore ratio of 380 kg/ton ore, leaching temperature of 190 °C, leaching time of 60 minutes, pulp density of 32.5%, and particle size of 150 μm). In the pressurized acid process, the nickel and cobalt extraction yields were only 74.5% and 72.2%, respectively [25]. The concentration of iron in the leachate is as high as 12.5 g/l. However, the selective leaching of the ore was achieved, with >85% yields for nickel and cobalt, while the iron extraction rate was 1.80 g/l. Atmospheric pressure acid leaching is sulphuric acid with optimal nickel, cobalt, and iron yields of 90%, as shown in Fig. 3 [26, 27].

The pressurized nitric acid leaching was carried out on five limonite laterite ores. Under optimal leaching conditions (nitric acid/ore 380 kg/t, particle size 150 μm (100%), and pulp density 32.5% at 190 for 60 min), the extraction yield for nickel and cobalt was 84.52% and 83.85%.

Meanwhile, pressurized nitric acid leaching was carried out on three laterites containing high magnesium with optimal washing conditions (nitric acid: ore is 800 kg: 1 tonne, particle size is 150 m (100%), and pulp density is 28.5% at 150 °C for 60 minutes), the average extraction yields of Ni and Co were 98.22% and 99.01%, respectively [28].

Similarly, in the pressure leaching process, the most frequently used acid during atmospheric pressure leaching is sulfuric acid [29]. There are many studies on leaching with hydrochloric acid, nitric acid, and organic acids as leaching materials to extract nickel from laterite nickel ores [26, 30, 31]. Atmospheric pressure sulphuric acid leaching extracting laterite ore with nickel content of 1.27% by weight and iron content of 39.93% by weight under ultrasonic and non-ultrasonic conditions at optimal leaching were found as follow: particle size of 74 m (95%), leaching temperature of 80 °C, sulphuric acid concentration of 190 g/l, solid/liquid ratio of 20%, leaching time of 2 hours, and stirring speed of 400 rpm [32]. Under the same conditions, the extraction of Ni and Fe reached 98.35% and 91.28% with an ultrasonic field activity that worked 4 minutes every 5 minutes [32]. In contrast, the extraction of nickel and iron was only 78.84% and 80.26% in the absence of ultrasonic [32].

2.3. Monosodium Glutamate Leaching

The effect of glutamate as a lixiviant was tested at concentrations of 0.5, 1 and 1.5 M. The pH of the solution was determined by the ratio of ammonia and glutamic acid. The increase in glutamate (added as glutamic acid) decreased the pH due to neutralization from 9.5 (1 M glutamate) to 8.3 (1.25 M) and 7.5 (1.5 M). A decrease in pH reduces the dissolution rate and maximum recovery of Ni. At lower pH, ammonia will be protonated and lose its ability as a synergist to form complexes with Ni [33]. Figure 4 shows the effect of the variation of molarity on nickel recovery, which indicates that MSG can be used as an alternative solvent in the nickel leaching process.

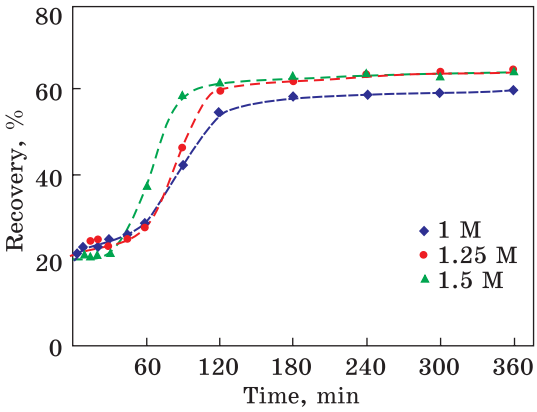

Fig. 4. Ni recovery using lixiviant ammonia–ammonium glutamate at different ammonia concentrations [33]

2.4. Purification Process

The cobalt/magnesium ratio is higher using 100% of Ionquest 290 and lower using 60% of Ionquest 290–92.9 and 22.7, respectively. The nickel/magnesium ratio was higher using 80% of Ionquest 290 and lower using 100% of Cyanex 272. With this result, the separation of cobalt from nickel-rich solutions was higher using 80% Ionquest 290 and 20% Cyanex 272, as shown in Table 1. However, nickel loss is lower using 60% Ionquest 290, which is 4.6%. The nickel concentration was higher after the solvent extraction experiment was conducted using 60% Ionquest 290–83.9 g/L. Authors of Ref. [34] studied the separation of cobalt from Ni-rich solutions using Cyanex 272. The separation of cobalt was 99.45% at 65 °C and pH 5.2, and there was no nickel loss [34]. For this reason, the results show that with concentrated solutions of nickel and cobalt, the use of synergism is beneficial. Iron can be separated using solvent extraction. However, cobalt loss occurs. In solution, the separation of iron by precipitation causes co-precipitation of Cu and Co due to the high concentration of Fe. There is separation of iron by precipitation because of its low concentration in solution (0.6 g/l) and synergism to recover vanadium using DEHPA and PC88A as organic extractants [35]. The results showed that the maximum nickel recovery used 80%

Table 1. **Concentrations of nickel, cobalt, and magnesium (g/l) in the aqueous phase of the experiment [36]**

Experiment	Ionquest 290, %	Ni, %	Co, %	Mg, %	Experiment	Ionquest 290, %	Ni, %	Co, %	Mg, %
1	100	74.9	0.03	1.5	4	40	73.7	0.06	1.1
2	80	78.9	0.02	0.7	5	20	77.4	0.04	1.0
3	60	83.9	0.1	1.4	6	0	78.2	0.2	2.1

Table 2. **The efficiency of leaching H_2SO_4 laterite LAI (Agios Ioannis laterite) (24 hours) and LEV (Evia Island laterite) (6 hours) under at pH is 0.75, temperature 90 °C, solid to liquid ration S/L = 30%, followed by the addition of LK (Castoria Laterite) to increase the pH to 1.8 (up to 48 hours), by comparing the selectivity of Ni to Fe, Mg, and Al using the respective ratios and concentrations in pregnant leach solution (PLS) [37]**

Laterite	pH	Ni, mg/l	Co, mg/l	Fe, mg/l	Ca, mg/l	Mg, mg/l	Al, mg/l	Ni/Fe	Ni/Mg	Ni/Al
LAI	0.75	1100	82	10300	595	1630	6040	0.11	0.68	0.18
LAI+LK	1.8	2220	124	1850	456	24100	2000	1.2	0.09	1.11
LEV	0.75	2770	119	10100	—	6510	4560	0.27	0.43	0.61
LEV+LK	1.8	2430	94	2710	—	19300	2520	0.9	0.13	0.96

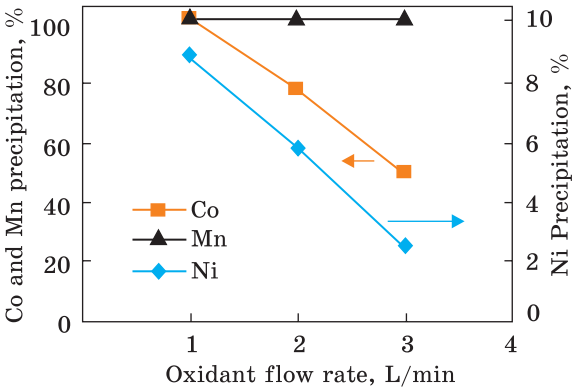

Fig. 5. Precipitation profiles for Co, Mn, and Ni as a function of the oxidant-gas flow rate at 25 °C, pH 5.0, and time of 2 hours [42]

Ionquest 290 and 20% Cyanex 272, where 99.1% extraction was possible [36].

In the precipitation process, the Ni/Fe ratio, which determines selectivity using the addition of pH method, Agios Ioannis laterite is leached separately at pH 0.75, is 0.11 with optimal results the higher the addition of pH as Table 2 [37]. The column-leaching test for low-grade Agios Ioannis ore (0.58% Ni) yielded a Ni/Fe ratio between 0.15 and 0.24 [38]. The applied a counter-current operating mode for HCl leaching from similar ores suppressing iron dissolution to 0.6%. However, this had a negative effect on the extraction of Ni and Co, which were limited to 55% and 63%, respectively [39]. Therefore, that precipitation is still not optimal in the purification process.

Another process, ozone precipitation, uses ozone as an alternative oxidant for persulphate due to a higher reduction potential, 2.08 V compared to 2.01 V [40]. Ozone can be generated on the spot and does not introduce sodium into the process. It can be seen the effect of O_3 on precipitation in Fig. 5; an increase in the gas flow rate resulted in a decrease in the rate of metal deposition. This is because the increase in gas rate to the corona ozone generator causes a decrease in the actual ozone content in the gas stream fed into the reactor. A similar experimental setup to study direct oxidative leaching of sphalerite concentrate using ozone as an oxidant reported that the ozone content in the gas stream was reduced from 6.72% by weight at 1 l/min to 3.78% by weight when the gas stream was reduced [41]. The oxidant rate in the ozone generator was increased to 3 l/min [42]. The results of this experiment thus reaffirm the critical role of ozone in the process of oxidative precipitation.

3. Pyrometallurgical Processes

The Caron process can be used for limonite ores or mixtures of limonite and saprolite. The ore is dried, and nickel is selectively reduced (along with cobalt and some iron) to metallic nickel at 700 °C. The metal is extracted by washing in an ammonia solution. The recovery of nickel and cobalt decreases with increasing saprolite, because nickel and cobalt

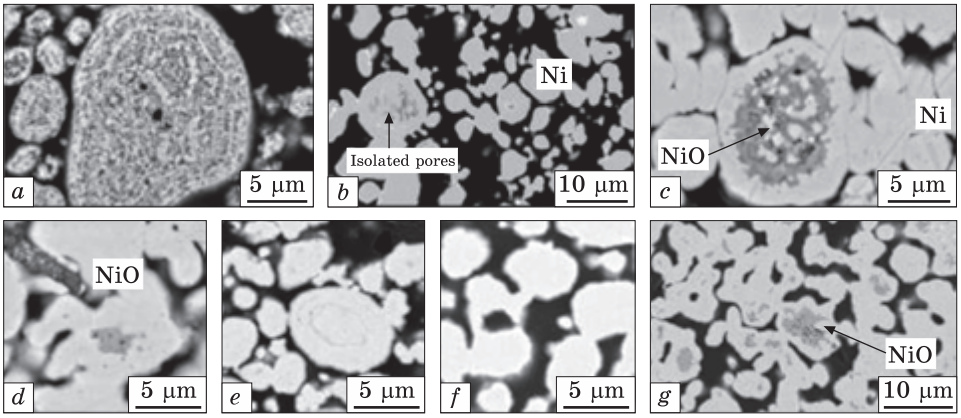

Fig. 6. Back scattering electron images of basic nickel carbonates' particles: (*a*) calcined in air at 900 °C and (*b*) reduced in 15% H_2–N_2 at 900 °C; pre-calcined in air at (*c*) and (*d*) 900 °C, (*e*) 700 °C, (*f*) 500 °C then reduced in 15% H_2–N_2 at 900 °C; and (g) reduced in 1.5% H_2–N_2 at 900 °C. All use a heating rate of 10 °C/min and a holding time of 30 min [43, 45]

are trapped in the silicate matrix and are challenging to reduce at this temperature [43]. The Caron process suffers from several weaknesses in the pyrometallurgical stage; hence, process modifications are needed.

3.1. Roasting

Calcination or roasting of laterite ore (Ni 1.26%, Fe 32.6%) has two functions, namely the removal of chemically bound water content during the goethite-hematite transformation and the reduction of volatiles in the reducing agent at a temperature of 350–700 °C [44]. As a result, it effectively reduces the chemically bound water content and all volatiles at 700 °C in the reducing agent. The transformation phase of the laterite ore during preheating and reduction with carbon monoxide to understand better the extent of its effect on the final reduction obtained [11]. The transformation of goethite to hematite and the decomposition of chlorite and serpentine were identified during preheating. In addition, nickel initiation is formed at a temperature of 900 °C and nickel products on the surface create a dense low-permeability layer and cover the unreduced NiO, as shown in Fig. 6 [43, 45].

3.2. Rotary Kiln-Electric Furnace

Nickel and iron ore are reduced to metal during the reduction process, and then the ferronickel product is separated from the slag through smelting. Producing nickel–sulphide matte in reduction smelting is a variation of extracting ferronickel during reduction and smelting by adding sulphur to the calcine feed at the smelting stage. Rotary kiln

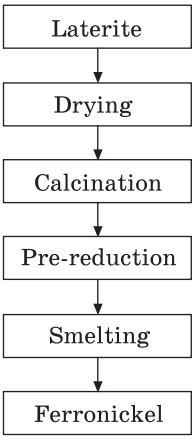

Fig. 7. Rotary kiln reduction-electric furnace smelting

reduction–smelting electric furnace is called RKEF; the main steps are drying, calcining, pre-reduction and melting. The flow chart of the RKEF process is depicted in Fig. 7. Due to the high free water content in laterite ores, the drying phase is justified in the RKEF process.

3.3. Selective Reduction

Selective reduction is a nickel extraction process using a temperature of 1000–1200 °C with low energy consumption followed by magnetic separation. It can be used to treat various types of laterite ores [46, 47]. In the reduction stage, nickel and iron are reduced to a metallic state at 1000–1200 °C. The ferronickel particles are separated from the slag in the magnetic separation step after the reduction results are pulverized. Nickel recovery rates are generally higher than 90%. The selective reduction separation process is carried out to increase the nickel content of ferronickel products. Nickel is reduced as much as possible, while the iron metallization must be restrained to achieve optimal nickel recovery and obtain ferronickel products with high nickel content. For selective reduction, iron must be metallized to some extent and act as a nickel carrier [13]. In addition, it is crucial to maximise the ferronickel particle size so that the ferronickel alloy can be recovered after refining and magnetic separation. The study of the increasing in silicate minerals was useful for increasing the nickel concentration by suppressing the reduction of iron oxide [48]. Other results showed that the addition of calcium sulphate strongly encouraged the growth of ferronickel particles. In addition, the level and rate of nickel recovery are influenced by the reductant dose. Magnetic-selective reduction separation process to treat laterite ore containing high iron (Ni 1.49%, Fe 34.69%) with the addition of sodium sulphate [46]. The ferronickel product with nickel content of 9.87% and nickel recovery rate of 90.9% was obtained from laterite ore, whose conditions included a reduction temperature of 1200 °C, 50 minutes, and an addition of 10% by weight of Na_2SO_4 and 2% of coal. Selective reduction of limonitic ore is with nickel content of 1.38% and iron content of 45.7% [14]. The effect of the addition of coal, sulphur, pyrite, and sodium sulphate, and temperature range of 1000–1200 °C on the selective reduction of limonite and saprolite was studied by [14]. The results showed that the addition of sulphur was more suitable for saprolite. In addition, the increase in the addition of carbon and sulphur and a higher reduction temperature will lead to the formation of fer-

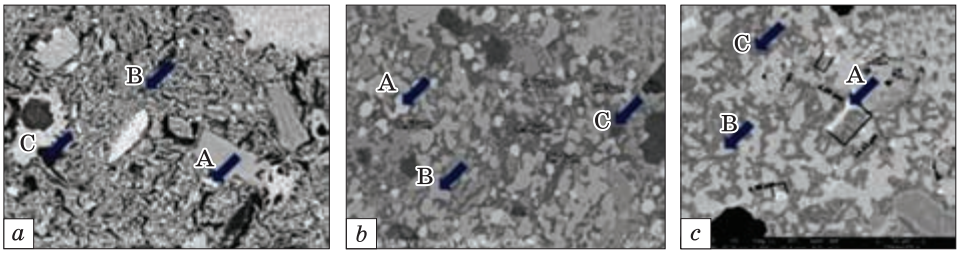

Fig. 8. Scanning electron microscopy images of the sample at a temperature of 1150 °C and the addition of 10% Na_2SO_4 for three reduction times: 60 (*a*), 90 (*b*), and 120 min (*c*) [54]

ronickel alloys, which reduce nickel content [14]. For the limonite sample, adding 4% of sulphur at a reduction temperature of 1100 °C for 1 hour resulted in ferronickel with average particle size of 1.59 μm, compared to 1.01 μm for the same conditions without sulphur addition. As for saprolite, the addition of sulphur seems to reduce the average size of ferronickel particles [14]. Therefore, the process of optimizing the selective reduction conditions and the selection of suitable additives for the different laterite ores are important. Na_2SO_4 can increase nickel laterite reduction by liberating iron and nickel from Ni/Fe substituted lizardite, increasing ferronickel particle size, and significantly reducing nickel content and recovery rate [2]. The troilite produced in the reduction system functions as an activating agent to accelerate the formation of the melt phase. During reduction, the aggregation of ferronickel particles occurs by completely suppressing iron metallization [2]. Na_2SO_4 can decompose into Na_2O and S in a reduced atmosphere, and Na_2SO_4 is also reduced to Na_2S [46]. S and Na_2S are useful for the selective reduction of Ni due to the formation of FeS. Na_2SO_4 reacts with CO and forms Na_2S, which then reacts with SiO_2 on the FeO surface to produce FeS and $Na_2Si_2O_5$ [25]. As a result, a thin layer of FeS is formed on the surface and blocks the contact between the reducing gas and FeO; so, iron reduction occurs. With the addition of Na_2SO_4, selective reduction of laterite nickel ore by H_2 in a fluidized reactor. Na_2SO_4 can control the kinetics of laterite ores and show catalytic activity when the temperature reaches more than 750 °C [49]. This shows that the reduction time affects the iron oxide reduction process. The sulphur from Na_2SO_4 will react with iron in laterite ore to form FeS, which can lower the fusion temperature and promote the growth of ferronickel particles [50, 51]. In other words, the Na_2SO_4 additive is advantageous for selective reduction by reducing the metallization ratio of iron through iron oxide sulphide. Reduction of low-grade nickel laterite ore with the addition of Na_2S, Na_2SO_4, and $CaSO_4$ [52]. Comparing the three additives, Na_2SO_4 can increase ferronickel growth and nickel content in ferronickel [52].

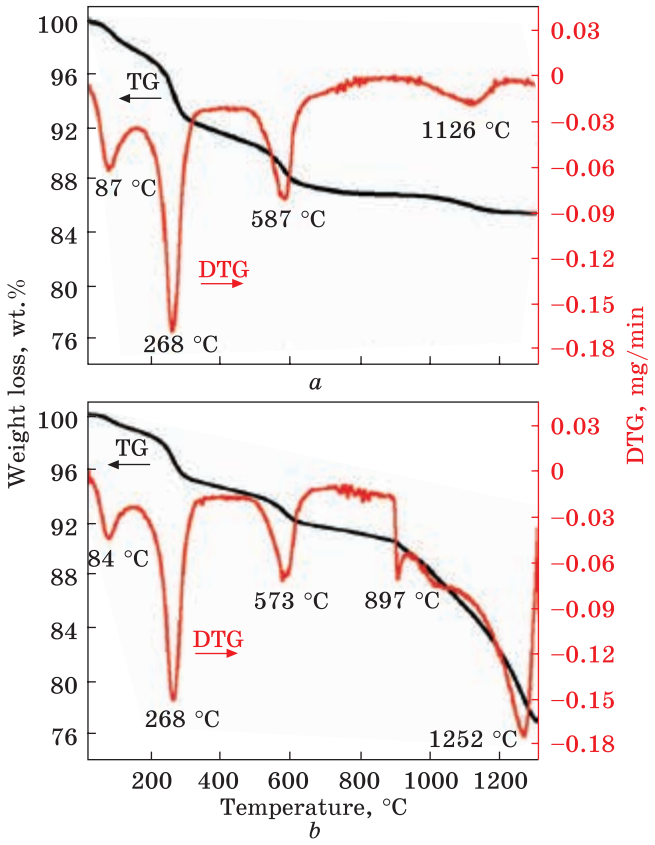

Fig. 9. Diagram of differential thermal analysis without (*a*) and with (*b*) Na_2SO_4 [59]

Figure 8 shows the effect of additives in the optimum separation of nickel and iron compared to the calcination process in Fig. 6 [53, 54]. Iron–nickel was formed optimally at 60 minutes at a temperature of 1150 °C, and additives were 10 wt.% Na_2SO_4.

Selective reduction is highly dependent on two aspects: the type and dose of reductant and additives. Suitable additives can strengthen selective reduction combustion, inhibit iron reduction, increase ferronickel particle size, and enhance the magnetic separation effect. The growth of ferronickel particles in the reduction-roasting step is quite important to determine whether the effective separation of ferronickel particles from impurities during the subsequent magnetic separation step can be achieved. The reduction temperature, time duration, and appropriate additives affect this. The selective reduction of nickel and the growth of ferronickel determine the nickel grade and the co-nickel recovery rate. The use of additives in the selective reduction process is carried out to increase the nickel content and recovery in the concentrate [53, 55]. One element that can be used as an additive is sulphur, in the form

Table 3. **Pre-research results on the effect of additives in selective reduction of laterite nickel ore [26, 53]**

Reductor (5%)	Additive, %						Grade, wt.%		Recovery, %	
	Na_2SO_4	NaCl	Na_2CO_3	$CaSO_4$	$CaCl_2$	CaCO	Ni	Fe	Ni	Fe
ACS — no sulphur	15						5.3	81.6	83.7	35.2
		5					2.1	66.7	72.8	63.2
			10				2.5	64.9	60.7	44.3
				15			3.31	64.74	53.46	29.01
					10		2.61	66.13	28.8	21.09
						15	1.952	63.39	50.98	45.89
Anthracite — high sulphur	15						15.1	60.6	65.5	7.3
		5					2.64	74.1	62.96	49.37
			5				2.67	83.23	55.55	83.23

of sodium sulphate, sodium sulphide, calcium sulphate [16, 46, 48, 50, 51, 56–58]. From the pre-research that has been done, sodium sulphate additive provides an increase in nickel content and optimal recovery compared to other additives, as shown in Table 3.

The addition of sodium sulphate can reduce Fe metallization due to the formation of FeS with a lower melting point (980 °C), thereby increasing the mass transfer rate of metal ions during the reduction process and causing ferronickel particles to aggregate [53, 56]. The large ferronickel particle size will increase the effectiveness of the ferronickel separation process against slag/impurities in the subsequent grinding process followed by magnetic separation.

As the differential thermal analysis results in Fig. 9 show, Na_2SO_4 can affect the rate of nickel diffusion at low temperatures of 1100–1250 °C and will reduce the formation of ferrous metal [59].

4. Synthesis of Nickel Nanoparticles and Their Application

In the last decade, nanotechnology has expanded the scope for researchers, manufacturers, and consumers in almost all sectors by enabling the engineering of functional systems at the nanoscale level, mainly in the form of nanoparticles [60]. Nanoparticles are raw materials used in nanotechnology [61]. As well as the bulk Ni-based alloys, Ni nanoparticles have received much attention due to their unique magnetic, chemical, and physical properties as well as their potential applications in various technological fields such as catalysis, batteries, ink for nanotube printing, and immobilization of biomolecules through the magnetic force of nickel nanoparticles [62–65]. Compared to other magnetic nanoparticles, Ni nanoparticles have great potential as catalysts in reactions and propellant and sintering additives in coatings, plastics, and fibres

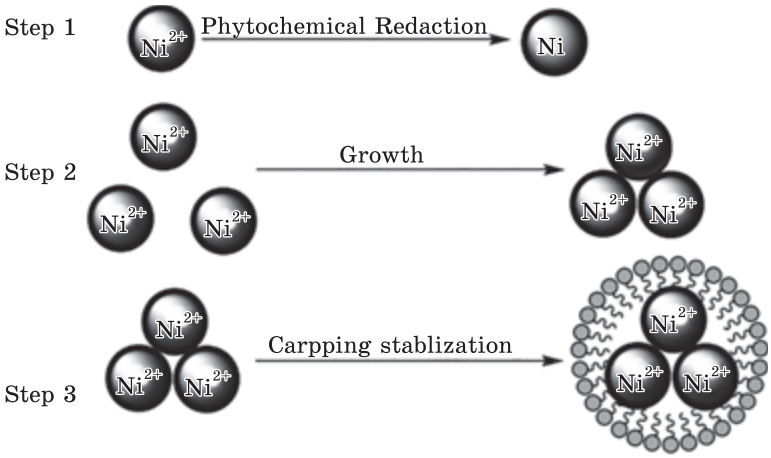

Fig. 10. Mechanism of nickel nanoparticles [70]

[66]. Due to its relative abundance in the Earth's crust, Ni is more cost-effective than most metals used as catalysts [67]. The electrical conductivity of Ni allows its use in several applications [68]. Nickel nanoparticles can be used as nanofluids in high purity, ultra-high purity, passivated, coated, and distributed [69]. The mechanism of nanoparticle can be seen in Fig. 10.

The synthesis of Ni nanoparticles is often associated with various challenges. Top-down synthesis methods and bottom-up synthesis protocols have traditionally been adapted to synthesis Ni nanoparticles. Top-down synthesis protocols include breaking down bulk materials into nanoscale materials [70]. The most widely used top-down nanoparticle synthesis methods are mechanical milling, laser ablation, nanolithography, thermal decomposition, and sputtering [71]. Mechanical milling is the most common method for producing nanoparticles, which varies among different top-down approaches. Mechanical milling is used during synthesis for milling and post-annealing of nanoparticles where many elements are ground in an inert atmosphere. Mechanical grinding is affected by plastic deformation, contributing to a particular shape, whereas fracture causes a decrease in particle size while cold welding increases particle size [72].

In conclusion of this section, note that a quasi-two-dimensional (2*D*) nickel hydroxide has been also grown [73, 74]. Among the family of currently known 2*D* materials (see, *e.g.*, [75–86] and references therein), 2*D* $Ni(OH)_2$ attracts the research interest as a promising material-candidate for application in a design of new devices in photonics, electronics, and optoelectronics [87].

5. Summary

Laterite is very difficult to extract because of its structure in hydroxide and complex impurities, which is different from nickel sulphide ores. The Caron process combines pyrometallurgy and hydrometallurgy. Pyrometallurgy uses roasting, which is ineffective to decrease magnesium and silica content. Therefore, process modification is needed like selective reduction to produce Ni concentrate, which Ni content ranges from 5 to 6 wt.% with a small quantity of magnesium and silica. Since the hydrometallurgy process, ammonia leaching, negatively affects the environment, a novel and green reagent such as MSG (monosodium glutamate) is proposed. MSG is also applied to attain high nickel and cobalt recovery. Another improvement is Ni purification by precipitation and nanoparticle synthesis, which results in nickel nanoparticles with 90–95 wt.% purity.

Acknowledgement. Authors thank for the financial support provided by the Ministry of Education, Culture, Research, and Technology of Directorate of Higher Education, Research, and Technology under research project PDD 2022 and contract No. NKB-968/UN2.RST/HKP.05.00/2022. The authors gratefully acknowledge the support of Materials Science Universitas Indonesia and the Research Centre of Mining Technology of the National Research and Innovation Agency of Indonesia for the research facilities.

REFERENCES

1. X. Ma, Z. Cui, and B. Zhao, Efficient utilization of nickel laterite to produce master alloy, *JOM*, **68**: 3006–3014 (2016); https://doi.org/10.1007/s11837-016-2028-5
2. J. Li, D. Xiong, H. Chen, R. Wang, and Y. Liang, Physicochemical factors affecting leaching of laterite ore in hydrochloric acid, *Hydrometallurgy*, **129**: 14–18 (2012); https://doi.org/10.1016/j.hydromet.2012.08.001
3. X. Lv, C. Bai, S. He, and Q. Huang, Mineral change of Philippine and Indonesia nickel lateritic ore during sintering and mineralogy of their sinter, *ISIJ Int.*, **50**: 380–385 (2010); https://doi.org/10.2355/isijinternational.50.380
4. S. Pournaderi, E. Keskinkılıç, A. Geveci, and Y. A. Topkaya, Reducibility of nickeliferous limonitic laterite ore from Central Anatolia, *Can. Metall. Quart.*, **53**: 26–37 (2014); https://doi.org/10.1179/1879139513Y.0000000099
5. J. Kim, G. Dodbiba, H. Tanno, K. Okaya, S. Matsuo, and T. Fujita, Calcination of low-grade laterite for concentration of Ni by magnetic separation, *Miner. Eng.*, **23**: 282–288 (2010); https://doi.org/10.1016/j.mineng.2010.01.005
6. C.A. Pickles, C.T. Harris, J. Peacey, and J. Forster, Thermodynamic analysis of the Fe–Ni–Co–Mg–Si–O–H–S–C–Cl system for selective sulphidation of a nickeliferous limonitic laterite ore, *Miner. Eng.*, **54**: 52–62 (2013); https://doi.org/10.1016/j.mineng.2013.03.029

7. C.A. Pickles, J. Forster, and R. Elliott, Thermodynamic analysis of the carbothermic reduction roasting of a nickeliferous limonitic laterite ore, *Miner Eng.*, **65**: 33–40 (2014);
https://doi.org/10.1016/j.mineng.2014.05.006
8. S. Al-Khirbash, Genesis and mineralogical classification of Ni-laterites, Oman Mountains, *Ore Geol. Rev.*, **65**: 199–212 (2015);
https://doi.org/10.1016/j.oregeorev.2014.09.022
9. N.M. Rice, A hydrochloric acid process for nickeliferous laterites, *Miner. Eng.*, **88**: 28–52 (2016);
https://doi.org/10.1016/j.mineng.2015.09.017
10. T. Agacayak, V. Zedef, and A. Aras, Kinetic study on leaching of nickel from Turkish lateritic ore in nitric acid solution, *J. Cent. South Univ.*, **23**: 39–43 (2016);
https://doi.org/10.1007/s11771-016-3046-8
11. E.N. Zevgolis, C. Zografidis, T. Perraki, and E. Devlin, Phase transformations of nickeliferous laterites during preheating and reduction with carbon monoxide, *J. Therm. Anal. Calorim.*, **100**: 133–139 (2010);
https://doi.org/10.1007/s10973-009-0198-x
12. A. Bunjaku, M. Kekkonen, K. Pietilä, and P. Taskinen, Effect of mineralogy and reducing agent on reduction of saprolitic nickel ores, *Trans. Inst. Min. Metall. C*, **121**: 156–165 (2012);
https://doi.org/10.1179/1743285512Y.0000000010
13. C.A. Pickles and R. Elliott, Thermodynamic analysis of selective reduction of nickeliferous limonitic laterite ore by carbon monoxide, *Trans. Inst. Min. Metall. C*, **124**: 208–2160 (2015);
https://doi.org/10.1179/1743285515Y.0000000009
14. R. Elliott, F. Rodrigues, C.A. Pickles, and J. Peacey, A two-stage thermal upgrading process for nickeliferous limonitic laterite ores, *Can. Metall. Quart.*, **54**: 395–405 (2015);
https://doi.org/10.1179/1879139515Y.0000000009
15. K. Quast, J.N. Connor, W. Skinner, D.J. Robinson, and J. Addai-Mensah, Preconcentration strategies in the processing of nickel laterite ores Part 1: Literature review, *Miner. Eng.*, **79**: 261–268 (2015);
https://doi.org/10.1016/j.mineng.2015.03.017
16. S.L. Chen, X.Y. Guo, W.T. Shi, and N. Li, Extraction of valuable metals from low-grade nickeliferous laterite ore by reduction roasting-ammonia leaching method, *Journal of Central South University of Technology*, **17**: 765–769 (2010);
https://doi.org/10.1007/s11771-010-0554-9
17. J. Kyle, Nickel laterite processing technologies – where to next? *ALTA 2010 Nickel/Cobalt/Copper Conf.* (24–27 May 2010, Perth, Western Australia).
18. A.D. Dalvi, W.G. Bacon, and R.C. Osborne, The past and the future of nickel laterites, *PDAC 2004 International Convention* (Trade Show & Investors Exchange, March 7–10, 2004).
19. M. Valix and W.H. Cheung, Effect of sulfur on the mineral phases of laterite ores at high temperature reduction, *Miner. Eng.*, **15**: 523–530 (2002);
https://doi.org/10.1016/S0892-6875(02)00069-9
20. B. Ma, C. Wang, W. Yang, F. Yin, and Y. Chen, Screening and reduction roasting of limonitic laterite and ammonia-carbonate leaching of nickel–cobalt to produce a high-grade iron concentrate, *Miner. Eng.*, **50**: 106–113 (2013);
https://doi.org/10.1016/j.mineng.2013.06.014

21. M.A.R. Önal and Y.A. Topkaya, Pressure acid leaching of Çaldağ lateritic nickel ore: an alternative to heap leaching, *Hydrometallurgy*, **142**: 98–107 (2014); https://doi.org/10.1016/j.hydromet.2013.11.011
22. J.A. Johnson, R.G. McDonald, D.M. Muir, and J. Tranne, Pressure acid leaching of arid-region nickel laterite ore Part IV: Effect of acid loading and additives with nontronite ores, *Hydrometallurgy*, **78**: 264–270 (2005); https://doi.org/10.1016/j.hydromet.2005.04.002
23. D.H. Rubisov, J.M. Krowinkel, and V.G. Papangelakis, Sulphuric acid pressure leaching of laterites-universal kinetics of nickel dissolution for limonites and limonitic/saprolitic blends, *Hydrometallurgy*, **58**: 1–11 (2000); https://doi.org/10.1016/S0304-386X(00)00094-3
24. K. Liu, Q. Chen, Z. Yin, H. Hu, and Z. Ding, Leaching kinetics of rare-earth elements from complex ores by acidic solutions, *Hydrometallurgy*, **125**: 125–136 (2012); https://doi.org/10.1007/978-3-319-95022-8_201
25. Z. Liu, T. Sun, X. Wang, and E. Gao, Generation process of FeS and its inhibition mechanism on iron mineral reduction in selective direct reduction of laterite nickel ore, *Int. J. Miner. Metall. Mater.*, **22**: 901–906 (2015); https://doi.org/10.1007/s12613-015-1148-1
26. F. Bahfie, A. Manaf, W. Astuti, F. Nurjaman, and U. Herlina, Tinjauan teknologi proses ekstraksi bijih nikel laterit, *Jurnal Teknologi Mineral dan Batubara*, **17**, No. 3: 135–152 (2021); https://doi.org/10.30556/jtmb.Vol17.No3.2021.1156
27. J. MacCarthy, J. Addai-Mensah, and A. Nosrati, Atmospheric acid leaching of siliceous goethitic Ni laterite ore: effect of solid loading and temperature, *Miner. Eng.*, **69**: 154–164 (2014); https://doi.org/10.1016/j.mineng.2014.08.005
28. B. Ma, W. Yang, B. Yang, C. Wang, Y. Chen, and Y. Zhang, Pilot-scale plant study on the innovative nitric acid pressure leaching technology for laterite ores, *Hydrometallurgy*, **155**: 88–94 (2015); https://doi.org/10.1016/j.hydromet.2015.04.016
29. P. Zhang, Q. Guo, G. Wei, L. Meng, L. Han, J. Qu, and T. Qi, Extraction of metals from saprolitic laterite ore through pressure hydrochloric-acid selective leaching, *Hydrometallurgy*, **157**: 149–158 (2015); https://doi.org/10.1016/j.hydromet.2015.08.007
30. Q. Guo, J. Qu, B. Han, P. Zhang, Y. Song, and T. Qi, Innovative technology for processing saprolitic laterite ores by hydrochloric acid atmospheric pressure leaching, *Miner. Eng.*, **71**: 1–6 (2015); https://doi.org/10.1016/j.mineng.2014.08.010
31. W. Astuti, T. Hirajima, K. Sasaki, and N. Okibe, Kinetics of nickel extraction from Indonesian saprolitic ore by citric acid leaching under atmospheric pressure, *Miner. Metall. Proc.*, **32**: 176–185 (2015); https://doi.org/10.1007/BF03402286
32. B. Wang, Q. Guo, G. Wei, P. Zhang, J. Qu, and T. Qi, Characterization, and atmospheric hydrochloric acid leaching of a limonitic laterite from Indonesia, *Hydrometallurgy*, **129**: 7–13 (2012); https://doi.org/10.1016/j.hydromet.2012.06.017
33. E. Prasetyo, F. Bahfie, and A.S. Handoko, Alkaline leaching of nickel from electric arc furnace dust using ammonia-ammonium glutamate as lixiviant, *Ni–Co 2021: The 5th Int. Symp. on Nickel and Cobalt, The Minerals, Metals & Materials Series* (2021); https://doi.org/10.1007/978-3-030-65647-8_14

34. J.A.B. Botelho, D.C.R. Espinosa, D. Dreisinger, and J.A.S. Tenyrio, Effect of iron oxidation state for copper recovery from nickel laterite leach solution using chelating resin, *Separation Science and Technology*, **55**, No. 4: 1–11 (2020); https://doi.org/10.1080/01496395.2019.1574828
35. Q. Shi, Y. Zhang, J. Huang, T. Liu, H. Liu, and L. Wang, Synergistic solvent extraction of vanadium from leaching solution of stone coal using D2EHPA and PC88A, *Separation and Purification Technology*, **181**: 1–7 (2017); https://doi.org/10.1016/j.seppur.2017.03.010
36. G.F.R. de Oliveira, J.A.B. Botelho, and J.A.S. Tenyrio, Separation of cobalt from the nickel-rich solution from HPAL process by synergism using organic extracts cyanex 272 and ionquest 290, *Tecnol. Metal. Mater. Miner.*, **16**, No. 4: 464–469 (2019); https://doi.org/10.4322/2176-1523.20191962
37. V. Miettinen, J. Mäkinen, E. Kolehmainen, T. Kravtsov, and L. Rintala, Iron control in atmospheric acid laterite leaching, *Minerals*, **9**: 404 (2019); https://doi.org/10.3390/min9070404
38. K. Komnitsas, E. Petrakis, O. Pantelaki, and A. Kritikaki, Column leaching of greek low-grade limonitic laterites, *Minerals*, **8**: 377 (2018); https://doi.org/10.3390/min8090377
39. C. Mystrioti, N. Papassiopi, A. Xenidis, and E. Komnitsas, Counter-current leaching of low-grade laterites with hydrochloric acid and proposed purification options of pregnant solution, *Minerals*, **8**: 599 (2018); https://doi.org/10.3390/min8120599
40. P. Vanýsek, *CRC Handbook of Chemistry and Physics; Electrochemical Series* (Eds. W.M. Haynes, D.R. Lide, and T.J. Bruno) (Taylor & Francis Group: 2017).
41. M.Z. Mubarok, K. Sukamto, Z.T. Ichlas, and A.T. Sugiarto, Direct sulfuric acid leaching of zinc sulphide concentrate using ozone as oxidant under atmospheric pressure, *Miner. Metall. Process.*, **35**: 133–140, (2018); https://doi.org/10.19150/mmp.8462
42. Z.T. Ichlas, M.Z. Mubarok, A. Magnalita, J. Vaughan, and A.T. Sugiarto, Processing mixed nickel-cobalt hydroxide precipitate by sulfuric acid leaching followed by selective oxidative precipitation of cobalt and manganese, *Hydrometallurgy*, **191**: 105185 (2020); https://doi.org/10.1016/j.hydromet.2019.105185
43. M.A. Rhamdhani, E. Jak, and P.C. Hayes, BNC. Part I Microstructure and phase changes during oxidation and reduction processes, *Metallurgical and Materials Transactions B*, **39**: 218–233 (2008); https://doi.org/10.1007/s11663-007-9124-4
44. E. Keskinkilic, S. Pournaderi, A. Geveci, and Y.A. Topkaya, Calcination characteristics of laterite ores from the central region of Anatolia, *J. S. Afr. I. Min. Metall.*, **112**: 877–882 (2012).
45. M.A. Rhamdhani, J. Chen, T. Hidayat, E. Jak, and P. Hayes, Advances in research on nickel production through the Caron process, *Proc. EMC 2009* (2009).
46. M. Jiang, T. Sun, Z. Liu, J. Kou, N. Liu, and S. Zhang, Mechanism of sodium sulphate in promoting selective reduction of nickel laterite ore during reduction roasting process, *Int. J. Miner. Process.*, **123**: 32–38 (2013); https://doi.org/10.1016/j.minpro.2013.04.005
47. X. Tang, R. Liu, L. Yao, Z. Ji, Y. Zhang, and S. Li, Ferronickel enrichment by fine particle reduction and magnetic separation from nickel laterite ore, *Int. J. Minerals, Metall. Mater.*, **21**: 955–961 (2014); https://doi.org/10.1007/s12613-014-0995-5

48. D.Q. Zhu, Y. Cui, K. Vining, S. Hapugoda, J. Douglas, J. Pan, and G.L. Zheng, Upgrading low nickel content laterite ores using selective reduction followed by magnetic separation, *Int. J. Miner. Process.*, **106**: 1–7 (2012); https://doi.org/10.1016/j.minpro.2012.01.003
49. J. Lu, S. Liu, J. Shangguan, W. Du, F. Pan, and S. Yang, The effect of sodium sulphate on the hydrogen reduction process of nickel laterite ore, *Miner. Eng.*, **49**: 154–164 (2013); https://doi.org/10.1016/j.mineng.2013.05.023
50. M. Rao, G. Li, X. Zhang, J. Luo, Z. Peng, and T. Jiang, Reductive roasting of nickel laterite ore with sodium sulphate for Fe–Ni production. Part I: Reduction/sulfidation characteristics, *Sep. Sci. Technol.*, **51**: 1408–1420 (2016); https://doi.org/10.1080/01496395.2016.1162173
51. M. Rao, G. Li, X. Zhang, J. Luo, Z. Peng, and T. Jiang, Reductive roasting of nickel laterite ore with sodium sulphate for Fe-Ni production. Part II: Phase transformation and grain growth, *Sep. Sci. Technol.*, **51**: 1727–1735 (2016b); https://doi.org/10.1080/01496395.2016.1166134
52. S. Zhou, B. Li, Y. Wei, H. Wang, C. Wang, and B. Ma, Effect of additives on phase transformation of nickel laterite ore during low-temperature reduction roasting process using carbon monoxide, *Drying, Roasting, and Calcining of Minerals*: 177–184, (2015); https://doi.org/10.1007/978-3-319-48245-3_22
53. F. Nurjaman, A. Rahmawaty, M.F. Karimy, B. Suharno, and D. Ferdian, The role of sodium-based additives on reduction process of nickel ore, *IOP Conf. Ser.: Mater. Sci. Eng.*, **478**: 012001 (2018); https://doi.org/10.1088/1757-899X/478/1/012001
54. F. Nurjaman, A. Sa'adah, and B. Suharno, Optimal conditions for selective reduction process of nickel laterite ore, *IOP Conf. Series: Mater. Sci. Eng.*, **523**: (2019); https://doi.org/10.1088/1757-899X/523/1/012068
55. A. Bunjaku, M. Kekkonen, P. Taskinen, and L. Holappa, Thermal behaviour of hydrous nickel–magnesium silicates when heating up to 750 °C, *Mineral Processing and Extractive Metallurgy*, **120**, No. 3: 139–146 (2011); https://doi.org/10.1179/1743285511Y.0000000011
56. G. Li, T. Shi, M. Rao, T. Jiang, and Y. Zhang, Beneficiation of nickeliferrous laterite by reduction roasting in the presence of sodium sulphate, *Minerals Engineering*, **32**: 19–26 (2012); https://doi.org/10.1016/j.mineng.2012.03.012
57. G.-J. Chen, J.-S. Shiau, S.-H. Liu, and W.-S. Hwang, Optimal combination of calcination and reduction conditions as well as Na_2SO_4 additive for carbothermic reduction of limonite ore, *Materials Transection*, **57**: 1560–1566 (2016); https://doi.org/10.2320/matertrans.M2016072
58. I. Setiawan, S. Harjanto, A. Rustandi, and R. Subagja, Reducibility of low nickel lateritic ores with presence of calcium sulphate, *Int. J. Eng. Technol.*, **14**: 56–66 (2014).
59. S. Yang, W. Du, P. Shi, J. Shangguan, S. Liu, C. Zhou, P. Chen, Q. Zhan, and H. Fan, Mechanistic and kinetic analysis of Na_2SO_4-modified laterite decomposition by thermogravimetry coupled with mass spectrometry, *PLOS ONE*, **11**, No. 6: 1–21 (2016); https://doi.org/10.1371/journal.pone.0157369
60. L.A. Paramo, A.A. Feregrino-Perez, R. Guevara, S. Mendoza, and K. Esquivel, Nanoparticles in agroindustry: applications, toxicity, challenges, and trends,

Nanomaterials, **10**, No. 9: 654–86 (2020);
https://doi.org/10.3390/nano10091654
61. R. Magaye and J. Zhao, Recent progress in studies of metallic nickel and nickel-based nanoparticles' genotoxicity and carcinogenicity, *Environ. Toxicol. Pharmacol.*, **34**, No. 3: 644–650 (2012);
https://doi.org/10.1016/j.etap.2012.08.012
62. I. Bibi, S. Kamal, A. Ahmed, M. Iqbal, S. Nouren, and K. Jilani, Nickel nanoparticle synthesis using camellia sinensis as reducing and capping agent: growth mechanism and photocatalytic activity evaluation, *Int. J. Biol. Macromol.*, **103**: 783–790 (2017);
https://doi.org/10.1016/j.ijbiomac.2017.05.023
63. Y. Cheng, M. Guo, M. Zhai, Y. Yu, and J. Hu, Nickel nanoparticles anchored onto Ni foam for supercapacitors with high specific capacitance, *J. Nanosc. Nanotechnol.*, **20**, No. 4: 2402–2407 (2020);
https://doi.org/10.1166/jnn.2020.17377
64. A.R. Abdel Fattah, T. Majdi, A.M. Abdalla, S. Ghosh, and I.K. Puri, Nickel nanoparticles entangled in carbon nanotubes: novel ink for nanotube printing, *ACS Appl. Mater. Interfaces*, **8**, No. 3: 1589–1593 (2016);
https://doi.org/10.1021/acsami.5b11700
65. M.M. Barsan, T.A. Enache, N. Preda, G. Stan, N.G. Apostol, and E. Matei, Direct immobilization of biomolecules through magnetic forces on Ni electrodes via Ni nanoparticles: applications in electrochemical biosensors, *ACS Appl. Mater. Interfaces*, **11**, No. **22**: 19867–19877 (2019);
https://doi.org/10.1021/acsami.9b04990
66. D. Hill, A.R. Barron, and S. Alexander, Comparison of hydrophobicity and durability of functionalized aluminium oxide nanoparticle coatings with magnetite nanoparticles-links between morphology and wettability, *J. Colloid Interface Sci.*, **555**: 323–30 (2019);
https://doi.org/10.1016/j.jcis.2019.07.080
67. Z. Bian, S. Das, M.H. Wai, P. Hongmanorom, and S. Kawi, A review on bimetallic nickel-based catalysts for CO_2 reforming of methane, *ChemPhysChem.* **18**, No. 22: 3117–3134 (2017);
https://doi.org/10.1002/cphc.201701166
68. A. Sagasti, V. Palomares, J.M. Porro, I. Orue, M.B. Sanchez-Ilarduya, and A.C. Lopes, Magnetic, magnetoelastic and corrosion resistant properties of (Fe–Ni)-based metallic glasses for structural health monitoring applications, *Materials*, **13**, No. 1: 57–70 (2019);
https://doi.org/10.3390/ma13010057
69. D. Wang, Y. Jia, Y. He, L. Wang, J. Fan, and H. Xie, Enhanced photothermal conversion properties of magnetic nanofluids through rotating magnetic field for direct absorption solar collector, *J. Colloid Interface Sci.*, **557**: 266–75 (2019);
https://doi.org/10.1016/j.jcis.2019.09.022
70. N.D. Jaji, H.L. Lee, M.H. Hussin, H.M. Akil, M.R. Zakaria, and M.B.H. Othman, Advanced nickel nanoparticles technology: from synthesis to applications, *Nanotechnol. Rev.*, **9**: 1456–1480 (2020);
https://doi.org/10.1515/ntrev-2020-010
71. A.M. Ealias and M. Saravanakumar, A review on the classification, characterisation, synthesis of nanoparticles and their application, *IOP Conf. Ser. Mater. Sci. Eng.*, **263**: 32019 (2017);
https://doi.org/10.1088/1757-899X/263/3/032019

72. O. Molnarova, P. Malek, J. Vesely, P. Minarik, F. Lukac, T. Chraska, The influence of milling and spark plasma sintering on the microstructure and properties of the Al7075 alloy, *Materials*, **11**, No. 4: 547–64 (2018); https://doi.org/10.3390/ma11040547
73. S. Ida, D. Shiga, M. Koinuma, and Y. Matsumoto, Synthesis of hexagonal nickel hydroxide nanosheets by exfoliation of layered nickel hydroxide intercalated with dodecyl sulfate ions, *J. Am. Chem. Soc.*, **130**, No. 43: 14038–14039 (2008); https://doi.org/10.1021/ja804397n
74. G. Li, X. Wang, H. Ding, and T. Zhang, A facile synthesis method for $Ni(OH)_2$ ultrathin nanosheets and their conversion to porous NiO nanosheets used for formaldehyde sensing, *RSC Adv.*, **2**: 13018–13023 (2012); https://doi.org/10.1039/C2RA22049K
75. A.G. Solomenko, R.M. Balabai, T.M. Radchenko, and V.A. Tatarenko, Functionalization of quasi-two-dimensional materials: chemical and strain-induced modifications, *Prog. Phys. Met.*, **23**, No. 2: 147–238 (2022); https://doi.org/10.15407/ufm.23.02.147
76. T.M. Radchenko, I.Yu. Sahalianov, V.A. Tatarenko, Yu.I. Prylutskyy, P. Szroeder, M. Kempiński, and W. Kempiński, The impact of uniaxial strain and defect pattern on magnetoelectronic and transport properties of graphene, *Handbook of Graphene: Growth, Synthesis, and Functionalization* (Eds. E. Celasco and A. Chaika) (Beverly, MA: Scrivener Publishing LLC: 2019), Vol. 1, Ch. 14, p. 451; https://doi.org/10.1002/9781119468455.ch14
77. P. Szroeder, I.Yu. Sagalianov, T.M. Radchenko, V.A. Tatarenko, Yu.I. Prylutskyy, and W. Strupiński, Effect of uniaxial stress on the electrochemical properties of graphene with point defects, *Appl. Surf. Sci.*, **442**: 185–188 (2018); https://doi.org/10.1016/j.apsusc.2018.02.150
78. P. Szroeder, I. Sahalianov, T. Radchenko, V. Tatarenko, and Yu. Prylutskyy, The strain- and impurity-dependent electron states and catalytic activity of graphene in a static magnetic field, *Optical Mater.*, **96**: 109284-1–5 (2019); https://doi.org/10.1016/j.optmat.2019.109284
79. T.M. Radchenko and V.A. Tatarenko, Statistical thermodynamics and kinetics of long-range order in metal-doped graphene, *Solid State Phenomena*, **150**: 43–72 (2009); https://doi.org/10.4028/www.scientific.net/SSP.150.43
80. T.M. Radchenko and V.A. Tatarenko, Kinetics of atomic ordering in metal-doped graphene, *Solid State Sciences*, **12**, No. 2: 204–209 (2010); https://doi.org/10.1016/j.solidstatesciences.2009.05.027
81. T.M. Radchenko and V.A. Tatarenko, A statistical-thermodynamic analysis of stably ordered substitutional structures in graphene, *Physica E: Low-Dimensional Systems and Nanostructures*, **42**, No. 8: 2047–2054 (2010); https://doi.org/10.1016/j.physe.2010.03.024
82. T.M. Radchenko, A.A. Shylau, and I.V. Zozoulenko, Conductivity of epitaxial and CVD graphene with correlated line defects, *Solid State Communications*, **195**: 88–94 (2014); https://doi.org/10.1016/j.ssc.2014.07.012
83. I.Yu. Sahalianov, T.M. Radchenko, V.A. Tatarenko, and Yu.I. Prylutskyy, Magnetic field-, strain-, and disorder-induced responses in an energy spectrum of graphene, *Annals of Physics*, **398**: 80–93 (2018); https://doi.org/10.1016/j.aop.2018.09.004

84. T.M. Radchenko, I.Yu. Sahalianov, V.A. Tatarenko, Yu.I. Prylutskyy, P. Szroeder, M. Kempiński, and W. Kempiński, Strain- and adsorption-dependent electronic states and transport or localization in graphene, *Springer Proceedings in Physics: Nanooptics, Nanophotonics, Nanostructures, and Their Applications* (Eds. O. Fesenko and L. Yatsenko) (Cham, Switzerland: Springer: 2018), Vol. **210**, Ch. 3, p. 25;
https://doi.org/10.1007/978-3-319-91083-3_3
85. T.M. Radchenko, V.A. Tatarenko, and G. Cuniberti, Effects of external mechanical or magnetic fields and defects on electronic and transport properties of graphene, *Materials Today: Proceedings*, **35**, Pt. 4: 523 (2021);
https://doi.org/10.1016/j.matpr.2019.10.014
86. I.Yu. Sagalianov, T.M. Radchenko, V.A. Tatarenko, and G. Cuniberti, Sensitivity to strains and defects for manipulating the conductivity of graphene, *EPL*, **132**: 48002 (2020);
https://doi.org/10.1209/0295-5075/132/48002
87. X.-L. Wei, Z.-K. Tang, G.-C. Guo, S. Ma, and L.-M. Liu, Electronic and magnetism properties of two-dimensional stacked nickel hydroxides and nitrides, *Sci. Rep.*, **5**: 11656-1–9 (20015);
https://doi.org/10.1038/srep11656

Received 31.05.2022;
in final version, 31.01.2023

Ф. Бахфі[1], *А. Манаф*[2], *В. Астуті*[1], *Ф. Нурджаман*[1],
Е. Прасетйо[1,3], *Й. Тріапріані*[1], *Д. Сусанті*[4]

[1] Дослідницький центр технології гірничих робіт,
Національна аґенція досліджень та інновацій Індонезії,
Південний Лампунґ, 35361 Лампунґ, Індонезія

[2] Кафедра фізики, факультет математики та науки,
Університет Індонезія,
16424 Депок, Західна Ява, Індонезія

[3] Кафедра хімічної технології,
Норвезький університет науки та технологій,
7491 Тронгейм, Норвегія

[4] Кафедра металурґії та матеріалознавства,
Факультет промислових технічних засобів та системотехніки,
Технологічний інститут Десятого листопада,
60111 Сурабая, Східна Ява, Індонезія

ВІД НІКЛЕВОЇ РУДИ ДО НАНОЧАСТИНОК Ni В ПРОЦЕСІ ЕКСТРАҐУВАННЯ: ВЛАСТИВОСТІ ТА ЗАСТОСУВАННЯ

Латеритова ніклева руда — мінеральна гірська порода, що містить залізоніклеві оксидні сполуки. Однією з технологій перероблення, запропонованої для оброблення руди, є процес Карона. Загалом процес Карона поєднує пірометалурґійну та гідрометалурґійну стадії. На пірометалурґійній стадії руду, змішану з відновником, нагрівають до 1800 °C у ротаційній обпалювальній електричній печі для перетворення оксиду залізоніклю в залізоніклевий стоп. На гідрометалурґійній стадії нікель селективно розчиняється за допомогою розчину (лужного) аміаку. Подальший процес спрямовано на виділення й очищення ніклю в розчині аміаку за допомогою екстракції розчинником та осадження. До недоліків пірометалур-

ґійної стадії в процесі Карона можна віднести високу енергомісткість, низьку економічну цінність і технічні проблеми, такі як частково розтоплений матеріал, що заважає подальшому процесу. Перебуваючи на гідрометалурґійній стадії, широке використання аміаку спричиняє вплив на навколишнє середовище. Для вирішення завдань пірометалурґійної стадії пропонується селективне відновлення. Селективне відновлення — це процес, що сприяє утворенню оксиду заліза для одержання високого вмісту ніклю в проміжному продукті з меншим споживанням енергії. До руди додають добавку для селективного пониження вмісту ніклю та пониження температури реакції. Задля вирішення впливу аміаку на навколишнє середовище пропонується нова та безпечніша хімічна речовина в якості заміни — глутамат Натрію. Як альтернативу методу Карона пропонується селективне відновлення в поєднанні з лужним вилуговуванням за допомогою глутамату Натрію. Далі використовується осадження для очищення ніклю, що приводить до одержання наночастинок Ni з чистотою у 90–95 мас.%.

Ключові слова: латерит, метод Карона, очищення, синтез, наночастинки ніклю.